REPORT DOCUMENTATION PAGE

Form Approved
OMB No. 0704-0188

1. REPORT DATE *(DD-MM-YYYY)*	2. REPORT TYPE	3. DATES COVERED *(From - To)*
23-02-2009	Final Technical	1 March 2006 - 30 November 2008

4. TITLE AND SUBTITLE
Towards High-Reynolds Number Quiet Flow in Hypersonic Tunnels

5a. CONTRACT NUMBER

5b. GRANT NUMBER
FA9550-06-1-0195

5c. PROGRAM ELEMENT NUMBER

6. AUTHOR(S)
Doyle D. Knight and Hadassah Naiman

5d. PROJECT NUMBER

5e. TASK NUMBER

5f. WORK UNIT NUMBER

7. PERFORMING ORGANIZATION NAME(S) AND ADDRESS(ES)
Department of Mechanical and Aerospace Engineering
Rutgers - The State University of New Jersey
98 Brett Road
Piscataway, New Jersey 08854

8. PERFORMING ORGANIZATION REPORT NUMBER
CCD 2009-1

9. SPONSORING/MONITORING AGENCY NAME(S) AND ADDRESS(ES)
Air Force Office of Scientific Research
875 North Randolph Street, Room 3112
Arlington, Virginia 22203

10. SPONSOR/MONITOR'S ACRONYM(S)

11. SPONSOR/MONITOR'S REPORT NUMBER(S)
AFRL-AFOSR-VA-TR-2016-0668

12. DISTRIBUTION/AVAILABILITY STATEMENT
Unclassified; Distribution Unlimited

13. SUPPLEMENTARY NOTES

14. ABSTRACT

The report summarizes a research program focused on two main issues related to the achievement of high Reynolds number quiet flow in hypersonic tunnels, namely, 1) automated optimal design of quiet hypersonic tunnels, and 2) tunnel startup in the presence of blunt models. In the former case, a fully automated optimal design methodology was developed to determine the optimal shape of the supersonic nozzle to achieve laminar flow on the nozzle walls and hence quiet flow in the test section. In the latter case, detailed time-accurate simulations were performed for a cone model of different angles in the Purdue Quiet Tunnel. Results demonstrated the limiting size of the model that permitted startup of the tunnel.

15. SUBJECT TERMS
Hypersonic, transition, wind tunnel, computational fluid dynamics, stability analysis

16. SECURITY CLASSIFICATION OF:			17. LIMITATION OF ABSTRACT	18. NUMBER OF PAGES	19a. NAME OF RESPONSIBLE PERSON
a. REPORT	b. ABSTRACT	c. THIS PAGE			Doyle Knight
U	U	U	UU	16	19b. TELEPHONE NUMBER *(Include area code)* 732 445 4464

Final Technical Report

Towards High-Reynolds Number Quiet Flow in Hypersonic Tunnels

AFOSR Grant FA9550-06-1-0195

Period of Grant: 1 March 2006 - 30 November 2008

Prof. Doyle D. Knight and Ms. Hadassah Naiman
Department of Mechanical and Aerospace Engineering
Rutgers - The State University of New Jersey
98 Brett Road
Piscataway, New Jersey 08854
Phone: 732 445 4464 · Fax: 732 445 3124
Email: doyleknight@gmail.com

Submitted to:
Dr. John Schmisseur
Air Force Office of Scientific Research
875 North Randolph Street, Room 3112
Arlington, Virginia 22203
Phone: 703 696 6962 · Fax: 703 696 8451
Email: John.Schmisseur@afosr.af.mil

23 February 2009

Abstract

The report summarizes a research program focused on two major issues related to the achievement of high Reynolds number quiet flow in hypersonic tunnels, namely, 1) automated optimal design of quiet hypersonic tunnels, and 2) tunnel startup in the presence of blunt models. In the former case, a fully automated optimal design methodology was developed to determine the optimal shape of the supersonic nozzle to achieve laminar flow on the nozzle walls and maximize the length of the region of quiet flow in the test section. In the latter case, detailed time-accurate numerical simulations were performed for a cone model of different angles in the Purdue Quiet Tunnel. Results demonstrated the limiting size of the model that permitted startup of the tunnel.

1 Introduction

Accurate prediction of the location and extent of boundary layer transition in hypersonic flight is both a critical parameter in hypersonic vehicle design and an unsolved problem. The location of transition affects estimates of aerodynamic heating, skin friction drag and other boundary layer properties. Transition experiments have been performed in conventional wind tunnels for decades; however, most of the experimental data obtained from these facilities are contaminated by the high levels of noise that radiate from the turbulent boundary layers normally present on the nozzle walls. These high noise levels can cause transition to occur at Reynolds numbers (based on arc length) which are an order of magnitude earlier than in flight [4], and can also affect parametric trends for transition [11].

Experimental hypersonic transition research in ground-based facilities requires quiet flow in the test section. This implies laminar flow on the test section walls. Schneider [13] reviewed the history and status of quiet flow hypersonic wind tunnels. Beckwith [5, 6] led the design and fabrication of quiet tunnels at NASA Langley. A quiet Mach 3.5 tunnel was successfully demonstrated at NASA Langley in the early 1980s, followed by a quiet Mach 6 hypersonic facility in the mid-1990s. The Boeing/AFOSR Mach 6 Quiet Tunnel (BAM6QT) at Purdue University was constructed during 1995-2001. It is designed to achieve quiet flow for stagnation pressures up to 150 psia (1000 kPa), corresponding to a unit Reynolds number of $3.4 \cdot 10^6$ ft^{-1} ($11 \cdot 10^6$ m^{-1}) for a stagnation temperature of 433 K at Mach 6. It is presently the only operational hypersonic quiet tunnel in the world [14].

The conventional approach to design of the supersonic nozzle for quiet hypersonic tunnels is trial-and-error. An initial design is obtained using the conventional method of characteristics [16] based upon an assumed length for the test section. The displacement thickness of the assumed laminar boundary layer on the nozzle wall is subtracted from the inviscid contour to define the actual shape. A linear stability or parabolized stability analysis is performed for the laminar boundary layer on the nozzle wall [7]. The location of transition is defined by the growth factor N in the stability analysis. The Mach cone emanating from this location (assuming a circular cross-section for test section) and the Mach cone emanating from the inviscid method of characteristics form a back-to-front double cone region which defines the quiet flow region in the test section. This is illustrated in Fig. 1 for the BAM6QT. This procedure is then repeated until the desired size of the quiet flow region in the test section is achieved. The obvious weakness of this approach is the use of trial-and-error to determine the optimal quiet flow region.

The first objective of the research program is the development of an automated optimal design methodology for quiet hypersonic tunnels. The trial-and-error approach is replaced with an automated methodology which determines the maximum quiet flow test section size. The methodology is described in Section 2.

An important concern for all quiet hypersonic tunnels is starting the tunnel in the presence of a test model. Although slender vehicles are the primary concern in many transition

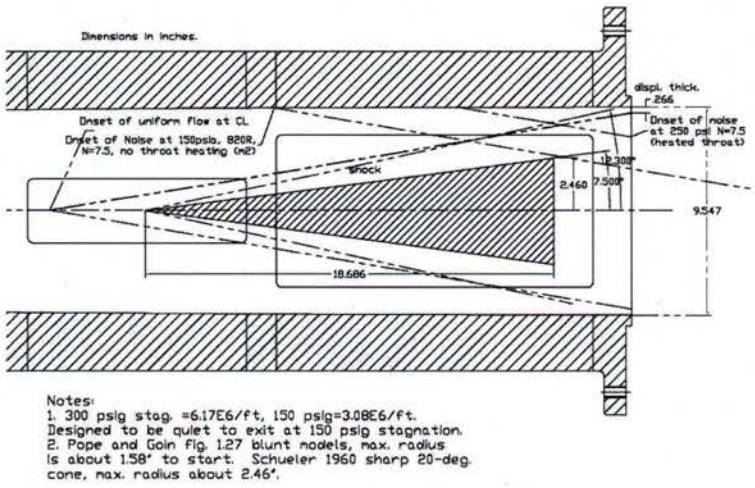

Figure 1: Test Section of Boeing-AFOSR Mach 6 Quiet Tunnel

experiments, blunt vehicles are also affected by transition [12]. Shocks emanating from the nose of the test cone and bow shocks from blunter models interact with the boundary layer on the tunnel wall. While disturbances in supersonic flow can only travel downstream, disturbances in the subsonic boundary layer flow in the test section can lead to separated flow upstream in the tunnel nozzle [17]. A laminar boundary layer is more likely to separate than turbulent boundary layer, and therefore shock wave boundary layer interactions are more likely to affect upstream flow in a quiet tunnel which has a laminar boundary layer on the nozzle wall. If the disturbance is too large, the tunnel will not start properly (*i.e.*, will not achieve uniform flow at the design Mach number upstream of the test model).

The second objective of the research is to evaluate the capability of the BAM6QT to start in the presence of test models of different bluntness and constant blockage. The test model is a cone with fixed base diameter (and hence, fixed blockage) and different cone angles (and hence, different shock strengths). The results are presented in Section 3.

2 Automated Design of Quiet Hypersonic Tunnels

The concept of automated optimal design of the test section for a quiet hypersonic tunnel is illustrated in Fig. 2. First, an inviscid contour is designed using the Method of Characteristics (MOC) with the Sivell's code [16]. Second, the compressible boundary layer is calculated and the inviscid contour is corrected for this boundary layer growth. Third, the corrected nozzle contour is provided to a grid generator and a mesh is created within the test section. Fourth, a Navier-Stokes code solves the steady-state flow using the grid. Fifth, this flowfield is input to a stability program that computes the most unstable disturbance and establishes

the point of transition along the nozzle contour using an assumed growth factor N. This transition point is used to evaluate the objective function which is the length of the quiet zone as measured on the test section centerline. This length is defined by the back-to-back cones created by the inviscid Sivell's code (the forward-facing cone) and the Mach cone emanating from the transition location (the backwards-facing cone) Lastly, the optimizer uses this value to create a response surface which is used to select a new set of parameters to use in the inviscid contour design.

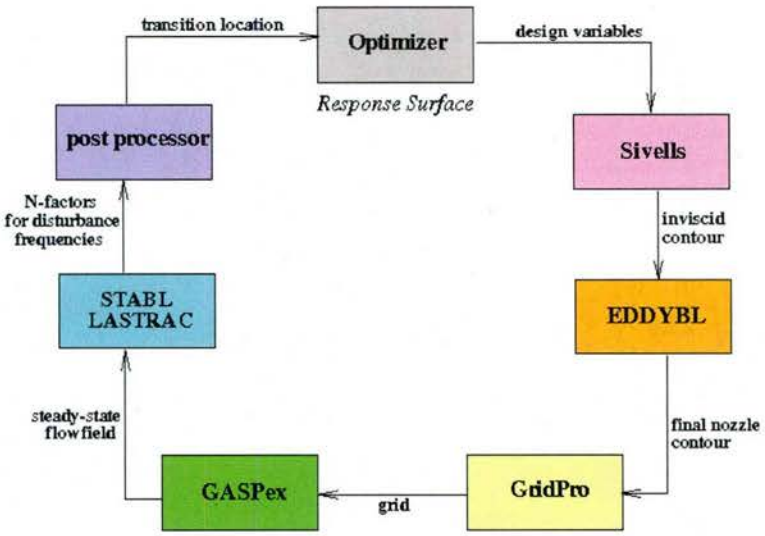

Figure 2: Automated Optimization Loop

The geometrical domain evaluated by the Sivells code is shown in Fig. 3. The computation starts at the throat using a transonic perturbation scheme. The transonic perturbation scheme is valid near Mach 1 and requires the throat radius of curvature. In this study, the BAM6QT coordinates are used for the contraction section upstream of the throat, and the throat radius of curvature specified in the Sivells input is smoothly connected to the upstream contraction section.

In addition to the throat radius of curvature, the input to the Sivells code includes the Mach number along the nozzle centerline for some distance (until the downstream parallel flow occurs). The code determines the appropriate centerline Mach number distribution that would result in a nozzle wall with continuous wall slope and curvature from the throat to the exit. The centerline Mach number distribution is based on polynomial functions that match the flowfield solutions at each flow region boundary. Once this distribution has been specified, a MOC procedure is used in an inverse design mode to determine an inviscid nozzle wall contour that produces the desired uniform exit flow. This inviscid contour can then be scaled to any particular size, based on a specified throat radius or exit radius.

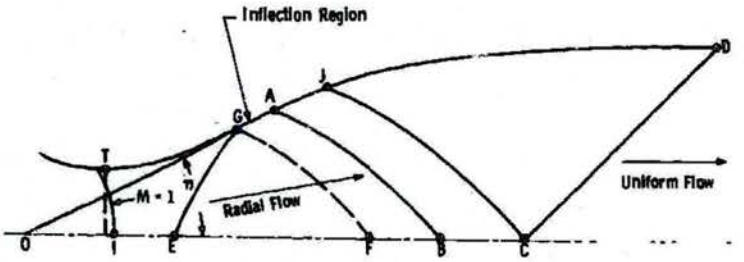

Figure 3: Radial Flow and Expansion Regions of Inviscid Contour[16]

The Sivells code is capable of generating nozzles with a region of radial flow between the initial expansion region and the inflection point, where the wall is shaped to turn the initial characteristcs so as to produce a uniform exit flow. This feature can be used to suppress the Goertler instability.

In summary, the Sivells code requires input of four parameters: RC (the ratio of throat radius of curvature to the throat radius), η (the expansion angle at the inflection points G and A in Fig. 3), $bmach$ (the Mach number at point B) and the design test section Mach number (taken to be $M = 6$ in this study).

The correction to the contour due to the compressible displacement thickness of the laminar boundary layer is calculated using using EDDYBL [19]. An example of the correction is shown in Fig. 4.

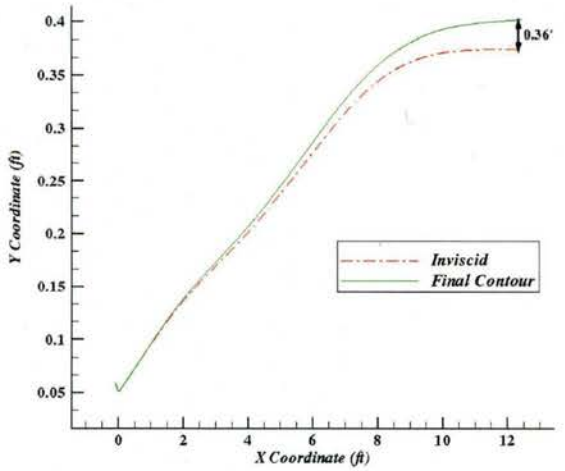

Figure 4: Example of Boundary Layer Correction for Mach 6 Test Section

The commercial software Gridpro [2] is used to generate the structured grid. GridPro is a general purpose elliptic mesh generator that creates a three dimensional, multi-block struc-

tured grid by a variationally-base method with an iterative updating scheme. The user input for Gridpro are the surface geometry and the block topology. It is important to note that the same topology definition is used during the optimization while the surface definition changes. An example of the grid topology is shown in Fig. 5

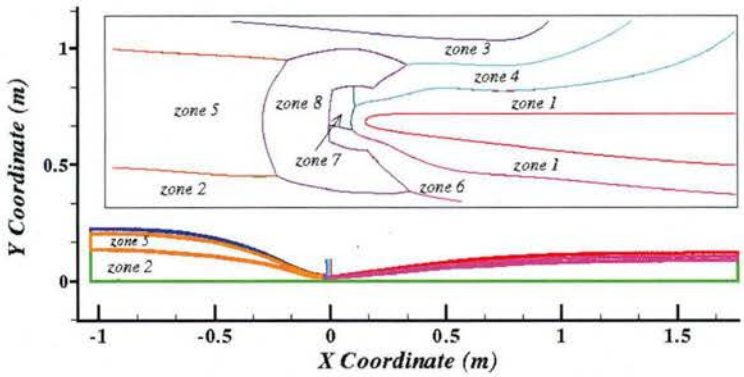

Figure 5: Example of Structured Grid

The flow solver is GASPex [3] (General Aerodynamic Simulation Program), a structured multiblock CFD solver for compressible viscous flow. The two dimensional axisymmetric Navier Stokes equations are solved using a finite volume spatial discretization. The optimization simulations use the steady-state formulation. The computations are second order accurate both in time and space.

The stability analysis is performed using the linear Parabolized Stability Equations (PSE) coupled with the e^N method to predict the location of laminar-to-turbulent transition. The code is LASTRAC [8]. Since the PSE constitute an initial boundary value problem, the wavenumber and eigenfunction at the starting location are obtained from linear stability theory (LST). A series of starting locations and frequencies are evaluated, and the growth factors calculated. An example is shown in Fig. 6. The furthest upstream location at which a particular disturbance reaches $N = 6$ is defined as the beginning of transition. The stability analysis incorporates the Goertler instability [8]. A separate *a posteriori* stability analysis is performed to examine the first- and second-mode instabilities using the STABL code [7]. It is observed that the Goertler instability dominates transition in nearly every case.

The computed length of the quiet zone in the test section (formed by the back-to-back cones) is the merit function of the optimization, and the objective is to determine the input parameters RC, η and $bmach$ for the Sivells' code that maximize the length of the quiet zone. The test section Mach number is fixed at $M = 6$. To improve the efficiency of the optimization, the individual results for each test section shape are parameterized as a Response Surface [10] which is used by the Multi-Objective Genetic Algorithm (MOGA) search engine to determine the optimal design. The optimization is performed using the modeFrontier [1] environment. The workflow diagram is shown in Fig. 7.

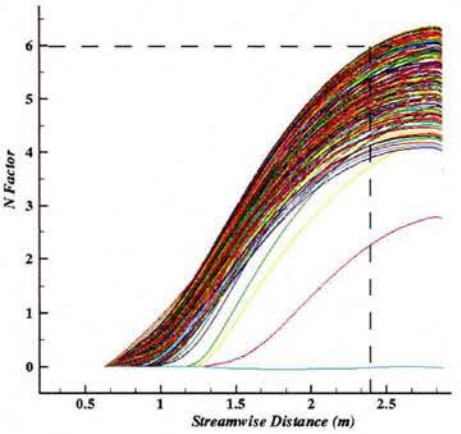

Figure 6: Example of Stability Analysis

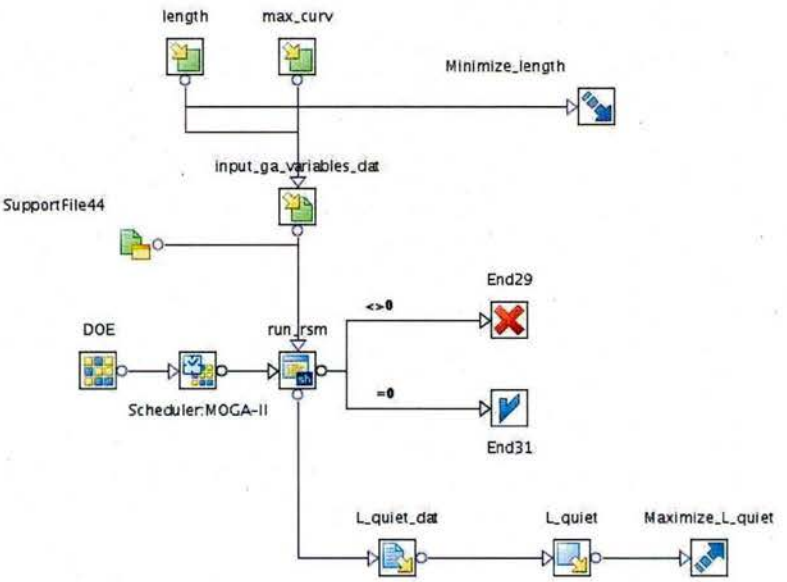

Figure 7: Workflow Diagram for Optimization

An example of an optimal design for a Mach 6 quiet tunnel is shown in Fig. 8 with the corresponding stability analysis using LASTRAC and STABL in Fig. 9. A unique feature is the compound curvature of the nozzle which results in a long section of quiet flow. This shape is unconventional, and illustrates the advantages of automated optimization (compared to trial-and-error) to discover new designs. The stability analyis for this design confirms that the transition is dominated by the Goertler instability.

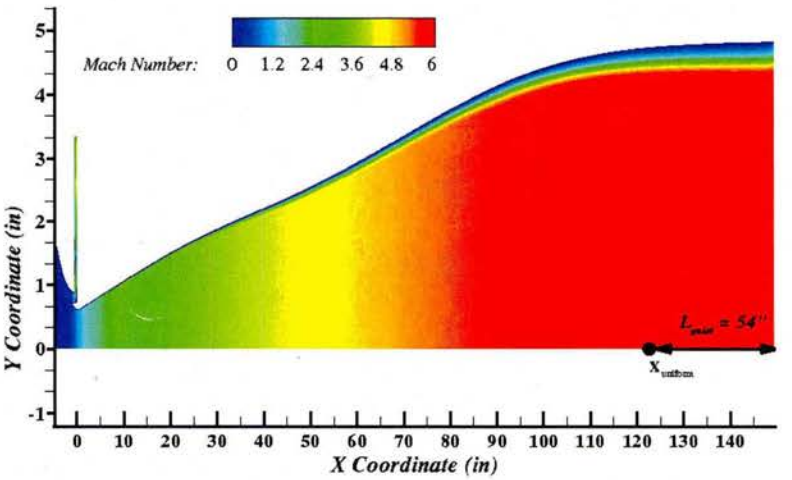

Figure 8: Optimal Design for Mach 6 Quiet Tunnel (vertical scale enlarged)

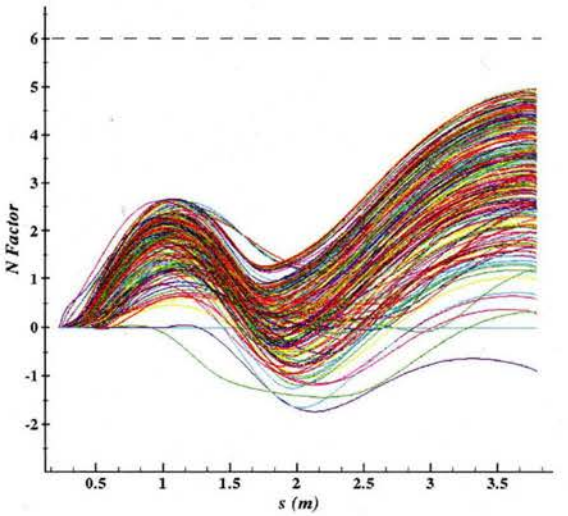

Figure 9: Stability Envelope for Optimal Mach 6 Design

3 Evaluation of Tunnel Startup for BAM6QT

The BAM6QT was modified [9] in 2006-2007 to incorporate an expanded test section (Fig. 10) for the purpose of testing larger and blunter models. In the original (unmodified) test section design (Fig. 1), the shock wave generated by the test model interacts with the laminar boundary layer on the nozzle wall. The concept of the expansion test section is to mitigate the shock wave laminar boundary layer interaction on the nozzle wall by substituting a shock

wave shear layer interaction. The abrupt expansion of the test section causes a separation of the incoming laminar boundary layer and the formation of a recirculation region and shear layer. The principal question is whether or not this concept would enable the tunnel to start with larger test models.

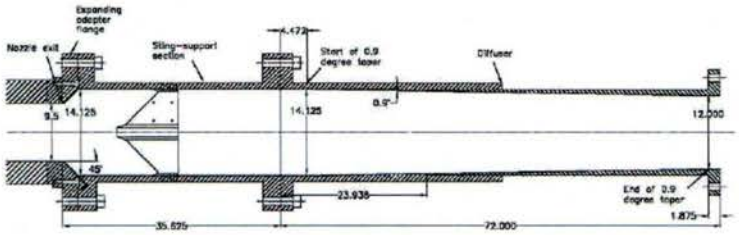

Figure 10: Expansion Section for Boeing-AFOSR Mach 6 Quiet Tunnel

The objective of the research is to examine the tunnel startup process for a test model in the expansion test section. A sharp cone at zero angle of attack was selected for the study. The cone geometry is characterized by the base diameter and cone angle. The base diameter determines the blockage ratio (*i.e.*, the ratio of projected model cross-sectional area to tunnel cross-sectional area), while the cone angle affects the strength of the shock wave generated by the model. The blockage ratio has traditionally been used to estimate the maximum allowable size for a test model [15]; however, it is widely recognized that the results on supersonic tunnel starting do not correlate simply with blockage due to the differences in the shock-boundary layer interaction generated by different models. Since there is no universally acceptable criteria for determining the effect of model size on tunnel starting for supersonic and hypersonic tunnels, a fixed blockage ratio (*i.e.*, fixed diameter) was chosen for simplicity. A 7° half-angle cone with a 5.5 inch base diameter is the largest model that can be started in the BAM6QT unmodified test section at zero angle of attack. Therefore, a fixed 5.5 inch base diameter was selected. The research examined cone half-angles ranging from 15° to 75° to determine the effect of the shock strength on tunnel startup.

A total of six computations were performed. One simulation was performed for the empty expansion test section, and five simulations were performed for cone half-angles of $15°, 20°, 30°, 50°$, and 75°. The empty expansion test section and the 15° half-angle cone have a 10° compression corner at the downstream end of the test section, but all other computations use a more gradual 1° compression based upon subsequent discussions with Prof. Steve Schneider.

The computational grids were generated with GridPro [2]. The domain for the empty section consists of one zone with 23,760 cells (100×241) and the domains for the cone cases consist of four zones and contain approximately 39,000 points. Grid clustering is performed with a stretching parameter of 1.105 and a first cell height of 10^{-4} ft along the wall and cone surfaces in order to resolve the boundary layers. Time-accurate simulations are performed with GASPex Version 4.1.0 [3], using an implicit dual time stepping algorithm with a time step of 10^{-6} s and 10 inner cycles. Each case runs until unstart occurs or until it appears

steady ($10 - 20$ ms physical time). The inviscid fluxes are discretized using Roe's scheme in conjunction with the Minmod limiter and MUSCL spatial reconstruction. The computations are second order accurate both in time and space. The inflow boundary condition is a user-specified flow with a boundary layer thickness corresponding to a laminar boundary layer that has been developing from the stagnation point at the bleed lip near the tunnel throat, and a uniform Mach 6.1 freestream flow. The boundary layer profile contains 50 points for the empty section and 40 points for the sections with cones, with a boundary layer thickness of 0.6 in (15 mm). The profile is calculated with EDDYBL [19], assuming a stagnation pressure of 90 psia, stagnation temperature of 433 K and choked flow at the throat.

The initial conditions are chosen to approximate the actual tunnel startup process. Warmbrod and Struck [18] describe the flow development in a Ludweig tube as a two stage process consisting of an expansion wave followed by a shock wave. The rupture of the diaphragm (downstream of the test section) generates an expansion fan that propagates upstream. This generates an initial downstream flow in the test section. When the expansion fan reaches the tunnel throat, the flow at the throat becomes sonic and an approximately normal shock wave is formed in the diverging section of the nozzle and propagated downstream. The shock eventually moves to the exit of the tunnel, accelerating the flow to Mach 6 within the test section. The initial conditions, along with the inflow conditions, create a shock wave that propagates into the computational domain in analogy to the actual tunnel startup process. The flow behind the shock wave is the proper tunnel design flow, and is determined by the inflow boundary condition. Thus, while the initial conditions do not precisely simulate the actual tunnel starting phenomena, they qualitatively model the second stage of the startup process (in which a shock wave travels through the test section accelerating the flow to design conditions) and provide the proper test section inflow conditions for the started tunnel.

The steady state (more precisely, the statistically stationary state) flowfield in the empty expansion test section is shown in Fig. 11. The numerical Schlieren is shown at $t = 20$ ms. The dark lines indicate a density gradient *i.e.*, shock wave, expansion fan or shear layer. The expansion test section generates a complex flowfield. A conical expansion fan occurs at the 45° corner and intersects the centerline. The recirculation region is separated from the core flow by a shear layer. Numerous weak shocks radiate from this shear layer and coalesce along the centerline downstream of the expansion section.

Figs. 12 and 13 display the numerical Schlieren image and Mach contours of the flowfield in the test section with a 15° half-angle cone at $t = 20$ ms (*i.e.*, at the statistically stationary state). A shear layer appears at the 45° expansion corner and a series of shocks turn the flow back at the 10° compression corner. A recirculation region is formed in the wake of the cone and in the expansion corner. The flowfield upstream of the cone is uniform (outside the boundary layer). It is therefore evident that the tunnel has successfully started.

Contours of streamwise velocity are shown in Fig. 14 for the 20° half-angle cone at $t = 20$ ms. The tunnel appears to have successfully started for this configuration. However, there is a very small upstream influence whereby the separation bubble spreads beyond the expansion

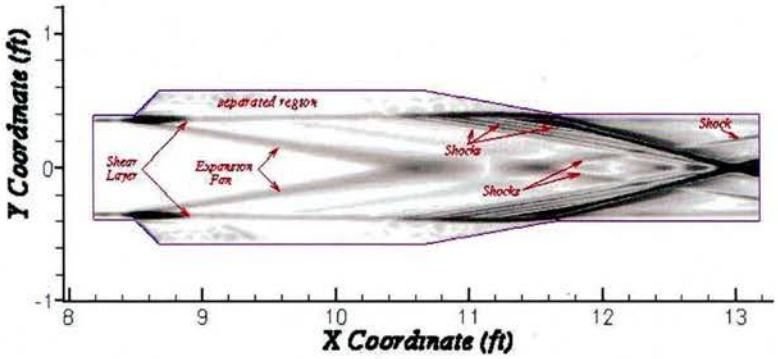

Figure 11: Numerical Schlieren of Empty Expansion Test Section

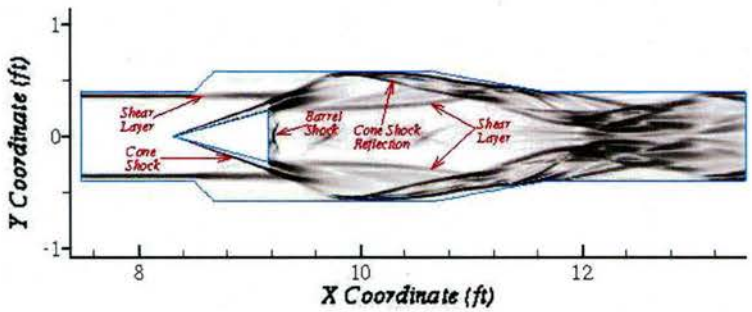

Figure 12: Numerical Schlieren of Expansion Test Section with 15° Cone

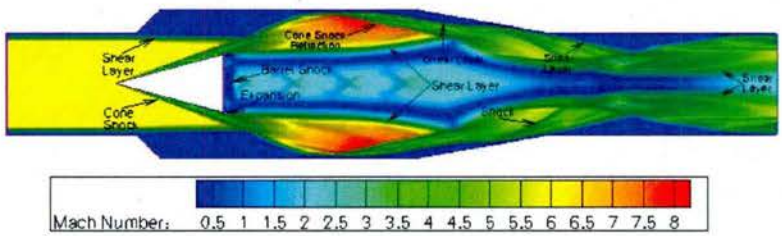

Figure 13: Mach Contours of Expansion Test Section with 15° Cone

corner. Unlike the blunter cones (see below), this separation bubble is steady and never reaches the upstream boundary.

The numerical Schlieren images for cone half-angles of 30°, 50° and 75° at 3 ms are shown in Figs. 15 to 17. In each case a separation bubble forms at the expansion corner and extends upstream. The separation bubble continues to grow until it reaches the inflow boundary. The streamwise velocity at the inflow boundary becomes negative. At this point, the results cease to be meaningful and the computation is stopped. These results imply that the tunnel

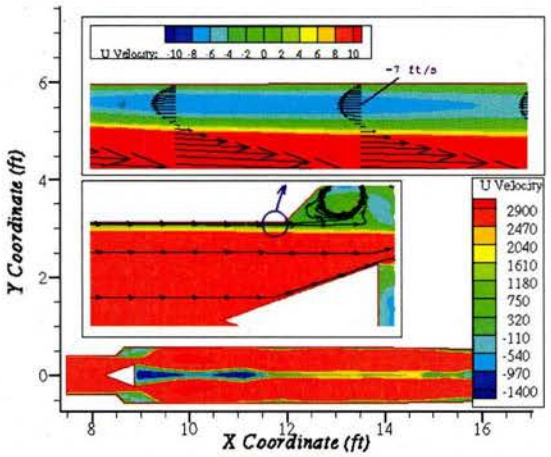

Figure 14: Streamwise Velocity Contours of Expansion Test Section with 20° Cone

cannot start with the 30°, 50° and 75° half-angle cones.

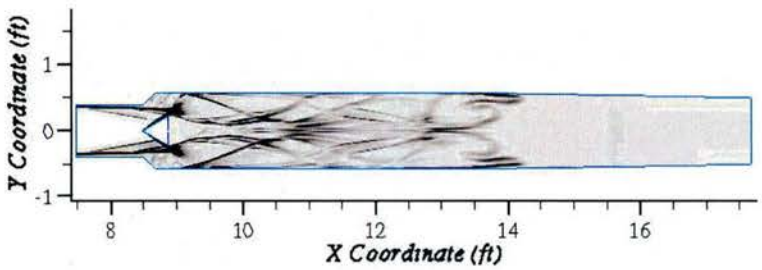

Figure 15: Numerical Schlieren of Expansion Test Section with 30° Cone at $t = 3$ ms

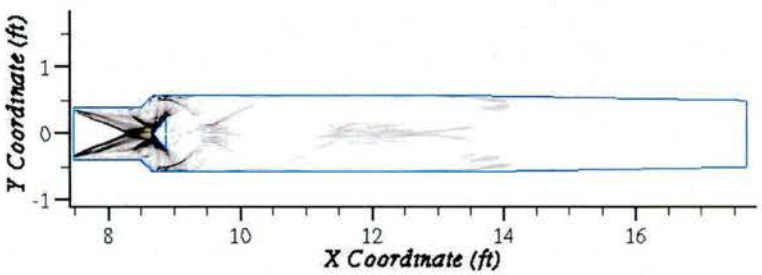

Figure 16: Numerical Schlieren of Expansion Test Section with 50° Cone at $t = 3$ ms

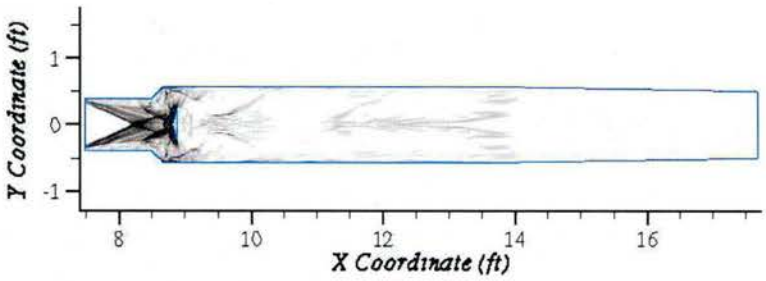

Figure 17: Numerical Schlieren of Expansion Test Section with 75° Cone at $t = 3$ ms

4 Publications

Naiman, H., Knight, D., Aradag, S., Juliano, T. and Schneider, S., "Performance Improvements in Boeing/AFOSR Mach 6 Quiet Wind Tunnel Based on CFD Predictions", Third International Symposium on Integrating CFD and Experiments in Aerodynamics, US Air Force Academy, Colorado Springs, CO, June 2007.

Naiman, H. and Knight, D., "Computational Redesign of the Test Section for the Boeing/AFOSR Mach 6 Quiet Tunnel", Second European Conference for Aerospace Sciences (EUCASS), Brussels, Belgium, July 2007.

Naiman, H., Knight, D., and Schneider, S., "Computational Redesign of the Test Section for the Boeing/AFOSR Mach 6 Quiet Tunnel", submitted to *Journal of Aerospace Engineering*, revision in progress.

5 Personnel

Principal Investigator: Prof. Doyle Knight

Graduate Student: Ms. Hadassah Naiman (PhD, Rutgers University, May 2009 (expected))

References

[1] modeFrontier Version 4 User's Manual. Esteco Research Laboratories, Padova, Italy.

[2] GridPro/az3000 User's Guide and Reference Manual. Program Development Corporation, White Plains, NY, 1996.

[3] GASP Version 4.2 User's Manual. Aerosoft, Inc., Blacksburg, VA, 2004.

[4] I.E. Beckwith, F.J. Chen, and T.R. Creel. Design requirements for the NASA Langley supersonic low-disturbance wind tunnel. Paper 86-0763, AIAA, 1986.

[5] Ivan E. Beckwith and Mitchel H. Bertram. A survey of NASA Langley studies on high-speed transition and the quiet tunnel. Technical Report TM-X-2566, NASA, July 1972. Citation 72N26239 in NASA Recon.

[6] Mitchel H. Bertram and Ivan E. Beckwith. NASA-Langley boundary layer transition investigations. In William D. McCauley, editor, *Boundary Layer Transition Study Group Meeting, Volume III, Session on ground test transition data and correlations*, August 1967. Paper 18 in the proceedings. The proceedings are available to US nationals from the Defense Technical Information Center as citation AD384006. The paper is citation 68X11187 in NASA RECON. The proceedings are Air Force Report No. BSD-TR-67-213, v. III, and Aerospace Corp. report no. TR-0158(S3816-63)-1, v. III.

[7] G. Candler and H. Johnson. STABL - A Modular Tool for Stability Analysis. https://stabl.aem.umn.edu.

[8] Chau-Lyan Chang. The Langley stability and transition analysis code (LASTRAC): LST, linear and nonlinear PSE for 2-D, axisymmetric, and infinite swept wing boundary layers. Paper 2003-0974, AIAA, January 2003.

[9] T. Juliano, R. Segura, M. Borg, K. Casper, M. Hannon, B. Wheaton, and S. Schneider. Starting issues and forward-facing cavity resonance in a hypersonic quiet tunnel. AIAA Paper No. 2008-3735, June 2008.

[10] R. Myers and D. Montgomery. *Response Surface Methodology.* Wiley Series in Probability and Statistics. John Wiley and Sons, New York, NY, 2002.

[11] H. Reed, R. Kimmel, D. Arnal, and S. Schneider. Drag prediction and transition in hypersonic flow. In *Sustained Hypersonic Flight.* AGARD, April 1997. Paper C15 in CP-600, vol. 3. Also appears as AIAA Paper 97-1818, June 1997.

[12] S. Schneider. Laminar-turbulent transition on reentry capsules and planetary probes. *Journal of Spacecraft and Rockets*, 43:1153–1173, 2006.

[13] S. Schneider. The development of hypersonic quiet tunnels. AIAA Paper No. 2007-4486, June 2007.

[14] S. Schneider, T. Juliano, E. Swanson, and M. Borg. High reynolds number laminar flow in the mach 6 quiet flow ludwieg tube. AIAA Paper No. 2006-3056, June 2006.

[15] K. Seablom, R. Soeder, D. Stark, J. Leone, and M. Henry. Nasa glenn 1-by 1-foot supersonic wind tunnel manual. Technical Report NASA TM-1999-208478, NASA Aeronautics and Space Administration, Glenn Research Center, April 1999.

[16] J.C. Sivells. A computer program for the aerodynamic design of axisymmetric and planar nozzles for supersonic and hypersonic wind tunnels. Technical Report AEDC-TR-78-63, Arnold Engineering Development Center, December 1978.

[17] C. Skoch, S. Schneider, and M. Borg. Disturbances from shock boundary layer interactions affecting upstream hypersonic flow. AIAA Paper No. 2005-4897, June 2005.

[18] J. Warmbrod and H. Struck. Application of the characteristic method in calculating the time-dependent, one-dimensional, compressible flow in a tube wind tunnel. Technical Report TM-X-53769, NASA, George C. Marshall Space Flight Center, Alabama, August 1968.

[19] D. Wilcox. *Turbulence Modeling for CFD.* DCW Industries, Inc., La Canada, California, third edition, 2006.